

The surface chemistry of Cu in the presence of CO₂ and H₂O

¹Xingyi Deng, ^{1,4}Albert Verdaguer, ¹Tirma Herranz, ¹Christoph Weis, ²Hendrik Bluhm, ^{1,3}Miquel Salmeron*

¹Materials Sciences Division, Lawrence Berkeley National Laboratory

²Chemical Sciences Division, Lawrence Berkeley National Laboratory

³Materials Science and Engineering Department, University of California, Berkeley, CA 94720, USA

E-mail: MBSalmeron@lbl.gov

*Author to whom correspondence should be addressed.

Abstract

The chemical nature of copper and copper oxide (Cu₂O) surfaces in the presence of CO₂ and H₂O at room temperature was investigated using ambient pressure x-ray photoelectron spectroscopy. The studies reveal that in the presence of 0.1 torr CO₂ several species form on the initially clean Cu, including carbonate CO₃²⁻, CO₂^{δ-} and C⁰, while no modifications occur on an oxidized surface. The addition of 0.1 ML Zn to the Cu results in the complete conversion of CO₂^{δ-} to carbonate. In a mixture of 0.1 torr H₂O and 0.1 torr CO₂, new species are formed, including hydroxyl, formate and methoxy, with H₂O providing the hydrogen needed for the formation of hydrogenated species.

Keywords: Cu, Zn/Cu, Cu₂O, CO₂, H₂O, surface chemistry, x-ray photoelectron spectroscopy.

⁴Current address: Institut Català de Nanotecnologia (ICN), 08193-Bellaterra, Barcelona. Spain

Introduction

The chemical reactions of copper with CO₂ and H₂O are at the basis of many fundamental processes in corrosion, catalysis and photochemistry of this widely used metal. Copper is used in pipes to transport water in urban environments during which it suffers from unwanted corrosion reactions. Copper is also used in electrical motors, in both rotor and brush electrodes. These motors operate often in environments containing CO₂ and H₂O. Here the problem is friction and wear of the brush surfaces, which depends on its reactivity towards these gases and on the passage of electrical current.^{1,2} Another important use of Cu is as a catalyst in methanol synthesis and water gas shift reactions, which also involve CO₂ and/or H₂O.³⁻⁵

It is not surprising therefore that the interaction of CO₂ with Cu surfaces has been extensively studied in past years. A considerable amount of analytical work has been performed under ultrahigh vacuum (UHV) conditions, using various surface sensitive techniques, such as x-ray photoelectron spectroscopy (XPS),⁶⁻⁸ high-resolution electron energy loss spectroscopy (HREELS),⁷ temperature programmed desorption (TPD),⁹ and surface enhanced Raman spectroscopy (SERS).¹⁰ In UHV, there are no measurable reactions of CO₂ with low Miller indices surfaces, i.e., Cu(111),¹¹ Cu(110),¹² and Cu(100),⁹ whereas activation of CO₂ via a chemisorbed CO₂^{δ-} species is favorable on stepped or polycrystalline surfaces, leading to a series of reactions.^{6,10,13} On the other hand, dissociation of CO₂ to CO and adsorbed oxygen on Cu(110) with dissociative reaction probabilities for CO₂ of ~10⁻⁹-10⁻¹¹ (per collision with the surface) was observed using Auger electron spectroscopy (AES) after exposures of 65-650 torr of CO₂ at 400-600 K in a high-pressure cell.¹⁴ While these studies have contributed considerably to establish the chemical nature of Cu surfaces exposed to CO₂, a more thorough understanding requires knowledge of the species formed *during operating conditions*, i.e., while exposed to realistic gas pressures of CO₂ or under condensed films of water.

In this paper we present the results of studies of several Cu-related surfaces, including Cu₂O, pure Cu, and Zn modified Cu in the presence of CO₂ and H₂O at room temperature and at pressures of 0.1 torr using ambient pressure x-ray photoelectron spectroscopy. Cuprous oxide (Cu₂O) is a common phase

of Cu and is formed with even small exposures to oxidizing gases. The study of Zn modified Cu surface is motivated by the fact that zinc is sometimes utilized as a binder in the brushes of electrical motors and is also because it is an important component of industrial methanol synthesis Cu catalysts (CuOx/ZnO).

Experimental

A sample of pure polycrystalline copper foil (99.999% from Alfa Aesar) was used in all experiments. The sample was pre-cleaned by ultrasonication in an acetone bath for 10 minutes, followed by another 10 minutes in methanol. Prior to the experiments the sample was electrochemically polished in a 50% phosphoric acid solution, using a negative Cu counter-electrode placed at about 1 cm distance with an applied voltage of 1.5 V for 5 minutes. After that the sample was rinsed with MiliQ water, dried with N₂ and introduced in the UHV chamber. Final cleaning consisted in several cycles of sputtering with Ar⁺ ions for 30 minutes followed by heating up to 800 K for 5 minutes.

On this surface only trace amounts of carbon, producing a peak at a binding energy (BE) of 284.7 eV and oxygen (less than 1%) at BE = 531.0 eV, were detected.

A Cu₂O surface was prepared by oxidation of the Cu foil *in situ*, following an exposure to 3×10^{-2} torr O₂ at 160 °C for 30 minutes. The XPS showed indeed a valence band shape characteristic of the oxide¹⁵. The band edge appears at 0.9 eV below the Fermi level, as expected from p-type Cu₂O, which has a band gap of 2 eV.¹⁶ The thickness of the oxide layer was estimated to be ≥ 1.5 nm based on depth profiling of the XPS peak intensities by variation of the incident photon energy.

Zinc (99.9997% from Alfa Aesar) was evaporated onto the cleaned Cu surface using a home-made evaporator. The evaporated film thickness was calibrated using a quartz crystal microbalance (QCM) and verified by comparing the Zn 3*p* and Cu 3*p* XPS peaks. The Zn coverage used in this study was estimated to be approximately 0.1 ML.

All XPS experiments were performed using a specially designed photoemission spectrometer that can operate at near-ambient pressures (up to several Torr) at undulator beamline 11.0.2. of the Advanced Light Source in Berkeley, USA.¹⁷ The C 1*s* and O 1*s* XP spectra were recorded at photon energies of

490 and 735 eV, respectively, corresponding to the same kinetic energy of 200 eV to ensure probing of the same depth. All spectra were collected at room temperature.

The XPS data analysis involved non-linear (Shirley) background subtraction and curve-fitting using mixed Gaussian-Lorentzian functions. The fitted peaks were constrained at positions known from the literature but with independent and variable full width at half maximum (FWHM) and intensities, as optimized by the program.

Results

Cu₂O in vacuum and in the presence of 0.1 torr CO₂

The C *1s* and O *1s* spectra of the Cu₂O surface prepared in UHV are shown in Figure 1. The surface is free of carbon as there was no detectable peak in the C *1s* region (Figure 1a). In the O *1s* region, the spectrum can be deconvoluted into two peaks: a major one at 530.2 eV, assigned to the lattice oxygen of Cu₂O, and a shoulder at 529.4 eV, assigned to surface oxygen.

CO₂ does not react with the Cu₂O surface as no adsorbed carbon species was detected after filling the chamber with 0.1 torr of CO₂. Specifically, no chemisorbed CO₂, carbonate (CO₃²⁻) or formate (HCOO⁻) species could be observed, as indicated by the absence of XPS peaks in the C *1s* region between 291-282 eV. A sharp peak at 292.7 eV is present due to the gas phase CO₂, excited by the x-ray beam above the sample. A small peak between 284 and 285 eV is assigned to residual contamination in the form of graphite or CH_x hydrocarbon fragments, referred as C⁰. In the O *1s* region, in addition to the lattice oxygen (530.2 eV) and surface oxygen (529.4 eV), a small peak appears at 531.1 eV and is assigned to OH (adsorbed hydroxyl).¹⁸ The presence of OH on the surface is due to the rise of H₂O background pressure upon introduction of 0.1 torr CO₂ into the chamber. It is known that OH is readily formed on surfaces in the presence of H₂O pressure as low as 1×10^{-7} torr.¹⁹ The peak at 536.3 eV is due to the gas phase CO₂.

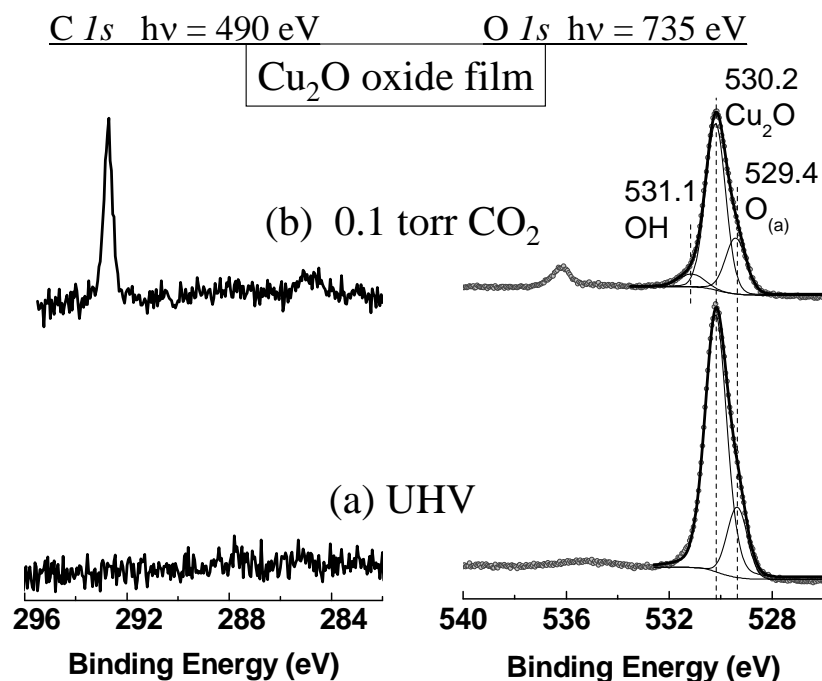


Figure 1. C *1s* and O *1s* XPS spectra of Cu₂O in (a) UHV; and (b) in 0.1 torr of CO₂ at room temperature. The main peak is due to lattice O in the oxide, at 530.2 eV binding energy (BE). A lower BE peak at 529.4 is assigned to surface oxygen. As can be seen the oxide surface is quite inert towards CO₂. The presence of a small surface hydroxyl (OH) peak at 531.1 eV upon introducing 0.1 torr CO₂ into the chamber is due to the rise in background pressure of H₂O. The peaks of O and C visible at 292.7 eV and 536.3 eV are due to gas phase CO₂. The x-ray energies were chosen such that all the photoelectrons had the same kinetic energy of approximately 200 eV. The Cu₂O, with a thickness ≥ 1.5 nm, was prepared by *in-situ* oxidation of a Cu foil.

Interestingly, we found that in the presence of CO₂ the incident x-rays or the emitted photoelectrons induce the formation of carbonate species on the surface. As seen in Figure 2, a C 1s peak at 289.3 eV, due to carbonate according to the literature,²⁰ appeared during spectrum acquisition that was not present in the fresh sample after the first data collection. As the spot illuminated by the x-rays was moved to a new fresh area, the C 1s peak at 289.3 eV disappeared in the first new cycle but again grew progressively with time. We will discuss this in more detail in the following section.

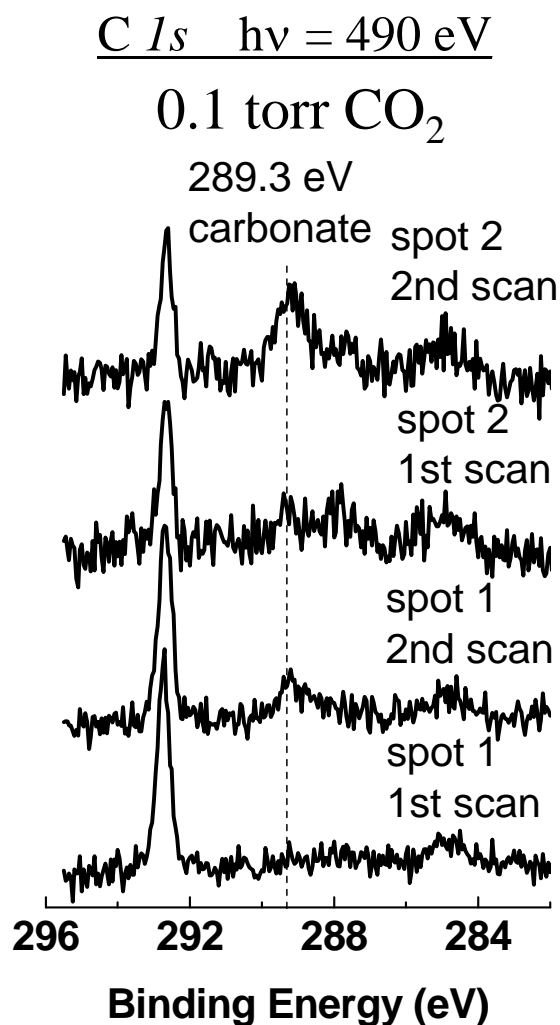


Figure 2. C 1s XPS spectra of Cu₂O in the presence of 0.1 torr CO₂ at room temperature, showing that the x-rays and/or the secondary photoelectrons induce carbonate formation on Cu₂O.

Clean Cu in the presence of 0.1 torr CO₂

The clean polycrystalline Cu surface is active towards CO₂, as three carbon species giving rise to C 1s peaks at 284.4, 288.4 and 289.3 eV, were observed in the presence of 0.1 torr CO₂ (Figure 3a). In the O 1s region the peaks corresponding to these species overlap substantially. The aggregate of peaks could be deconvoluted into 4 components at 529.8, 530.8, 531.4, and 531.9 eV. On the basis of our data and in comparison with the literature, we assign the C 1s peak at 289.3 eV and O 1s peak at 531.9 eV to a carbonate species; the C 1s peak at 288.4 eV and O 1s peak at 531.4 eV to chemisorbed, negatively charged CO₂ (CO₂^{δ-}); and the C 1s peak at 284.4 eV to a C⁰ species, as summarized in Table 1. Apart from C⁰, chemisorbed CO₂ constitutes the largest component of the surface species, its concentration being more than 4 times larger than that of the carbonate. After heating to 250°C however, all peaks in the 286-290 eV regions of the XPS disappear, indicating that carbonate and chemisorbed CO₂ are desorbed or decomposed at this higher temperature.

Table 1. XPS binding energies for carbon species found on Copper surfaces

	Carbonate		CO ₂ ^{δ-}		Formate		Methoxy		C ⁰		Ref.
	(eV)		(eV)		(eV)		(eV)		(eV)		
	C1s	O1s	C1s	O1s	C1s	O1s	C1s	O1s	C1s		
Cu ₂ CO ₃ (OH) ₂	289.1										20
Cu(poly)			289	531.4					285		6
Cu(poly)					287.7	531.4	285.2	530.2			21
Cu(poly)	289.3	531.9	288.4	531.4	287.3		285.2		284.4		This study

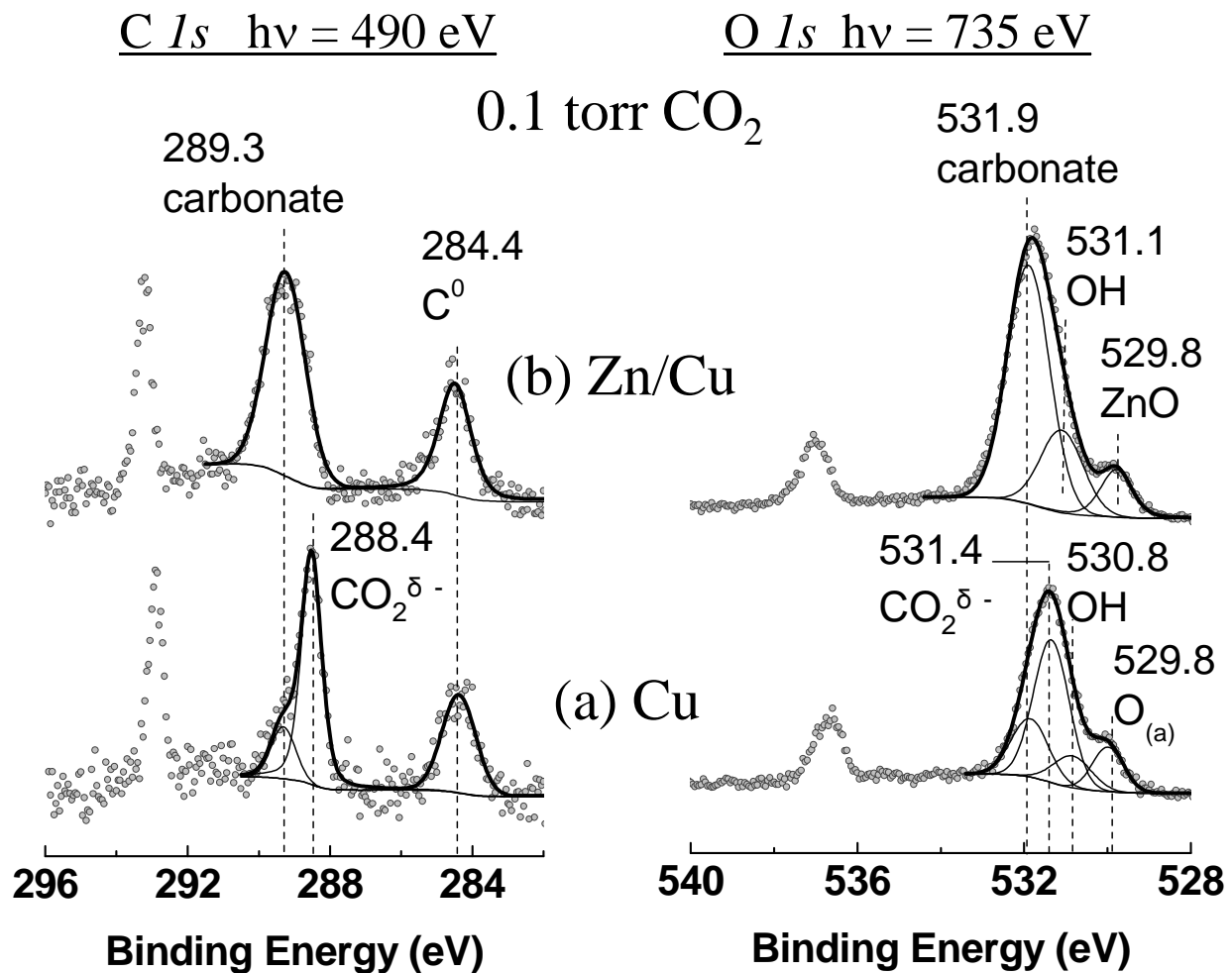


Figure 3. C 1s and O 1s XPS spectra of (a) pure Cu and (b) Zn/Cu (0.1 ML Zn) in the presence of 0.1 torr of CO_2 at room temperature. Three carbon species were identified on Cu: carbonate (CO_3^{2-}) at 289.3 eV, chemisorbed CO_2 ($\text{CO}_2^{\delta-}$) at 288.4 eV, and graphitic and/or hydrogenated C residues (C^0) at 284.4 eV. On the zinc covered Cu surface carbonate is formed instead of $\text{CO}_2^{\delta-}$. In the oxygen region, the species identified on Cu were carbonate (CO_3^{2-}) at 531.9 eV, chemisorbed CO_2 ($\text{CO}_2^{\delta-}$) at 531.4 eV, surface hydroxyl (OH) at 530.8 eV, and chemisorbed oxygen at 529.8 eV. On Zn/Cu, the peak due to carbonate (CO_3^{2-} , 531.9 eV) dominates the spectrum.

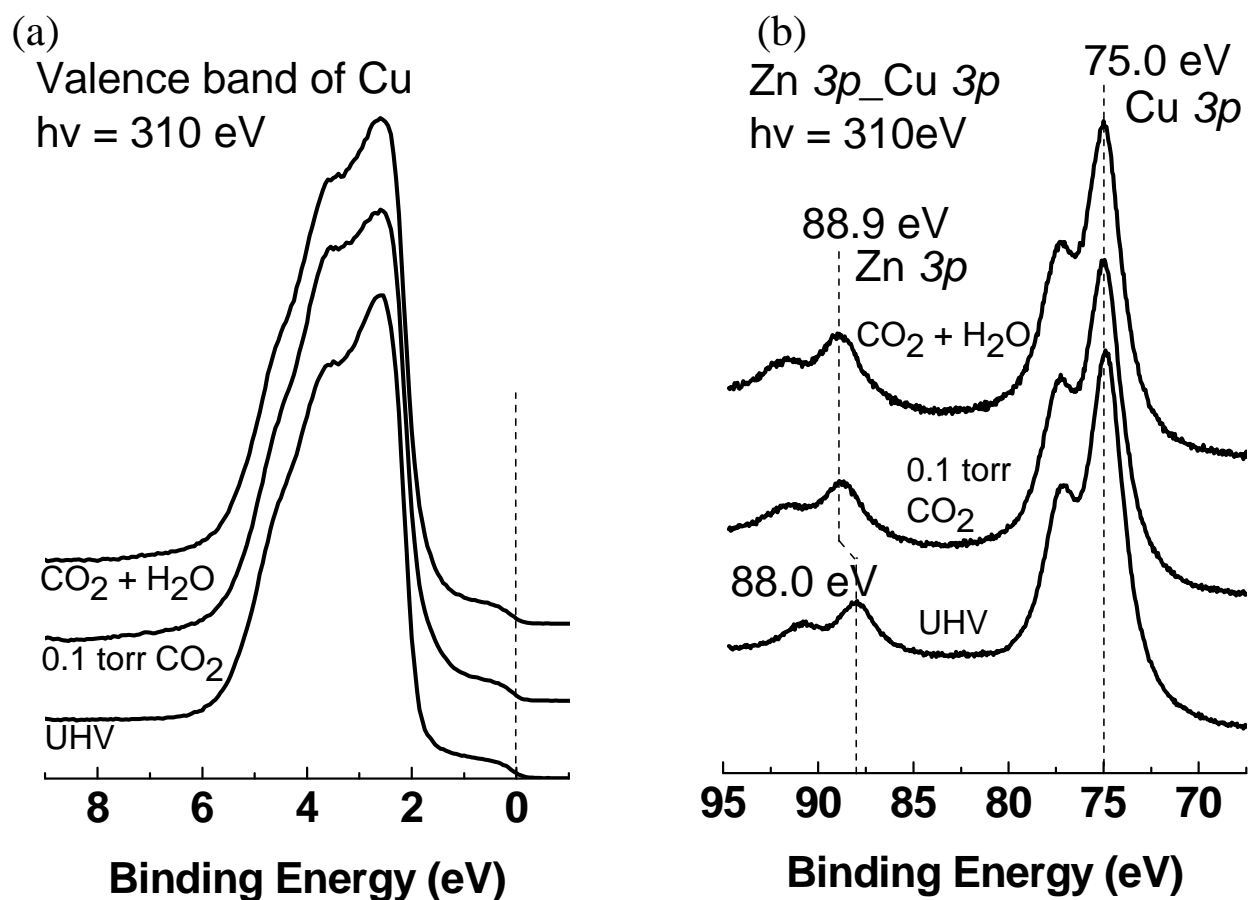


Figure 4. (a) Valence band region of pure Cu, and (b) Zn 3p and Cu 3p XPS spectra of Zn/Cu (0.1 ML Zn) in UHV, 0.1 torr CO₂, and 0.1 torr CO₂ + 0.1 torr H₂O at room temperature. These results show that CO₂ or CO₂ + H₂O do not oxidize pure Cu, as shown by the nonzero intensity at the Fermi edge, characteristic of the metallic surface. Zn however was oxidized in CO₂ or CO₂ + H₂O, as shown by a binding energy shift of +0.9 eV of the Zn 3p peaks.

The O 1s peaks at 530.8 and 529.8 eV are assigned to OH and chemisorbed oxygen, respectively. The gas phase CO₂ contributes to the C 1s and O 1s peaks at 292.9 and 536.7 eV, respectively.

There is no evidence for the formation of Cu₂O. Specifically, the valence band spectrum of Cu in the presence of 0.1 torr CO₂ is essentially the same as that of Cu in UHV (Figure 4a). The valence band spectrum clearly shows nonzero intensity at the Fermi edge, which is characteristic of a metallic surface.

This observation is consistent with the absence of the lattice oxygen peak characteristic of Cu₂O (BE = 530.2 eV) in the O *1s* region and the assignment of O *1s* peak at 529.8 eV to chemisorbed oxygen.

Zn/Cu in the presence of 0.1 torr CO₂

The presence of 0.1 ML of Zn on the Cu surface produces significant changes in the surface chemical composition upon exposure to 0.1 torr CO₂ (Figure 3b). Chemisorbed CO₂, the largest component on the clean Cu surface, is replaced by carbonate, which produces the major peak in the C *1s* region at 289.3 eV, in agreement with literature values.²⁰ Accordingly, the peak at 531.9 eV due to O in the carbonate dominates in the O *1s* region as well. Peaks due to CO₂^{δ-} are absent in both C *1s* (288.4 eV) and O *1s* (531.4 eV) regions. No measurable change was observed for C⁰ which remains at 284.4 eV.

Because of the rise of H₂O background pressure after introducing 0.1 torr of CO₂ in the chamber, OH is again present on the surface, producing the O *1s* peak at 531.1 eV. Similar to the observation on clean Cu, an O *1s* peak at 529.8 eV is detected. However, we assign this peak to O in ZnO as the binding energy of the Zn *3p* peak shifts + 0.9 eV in the presence 0.1 torr CO₂ (Figure 4b), indicating the oxidation of Zn.

Cu and Zn/Cu in the presence of 0.1 torr CO₂ + 0.1 torr H₂O

The addition of water to the gas phase produces changes in the chemical composition of both Cu and Zn/Cu. The C *1s* spectra of Cu and Zn/Cu in the presence of 0.1 torr CO₂ and 0.1 torr H₂O are shown in Figure 5a and b. The spectrum of the Cu surface could be deconvoluted into five peaks that we assign to carbonate (289.3 eV), CO₂^{δ-} (288.4 eV), formate (287.3 eV),^{21,22} methoxy (–O–CH₃) (285.2 eV)²¹ and C⁰ (284.4 eV), respectively. On the Zn/Cu surface, four species were observed: carbonate (289.3 eV), formate (287.3 eV), methoxy (285.2 eV) and C⁰ (284.4 eV). The two new species, methoxy and formate, are due to the reaction of CO₂ with H₂O since they both contain hydrogen.

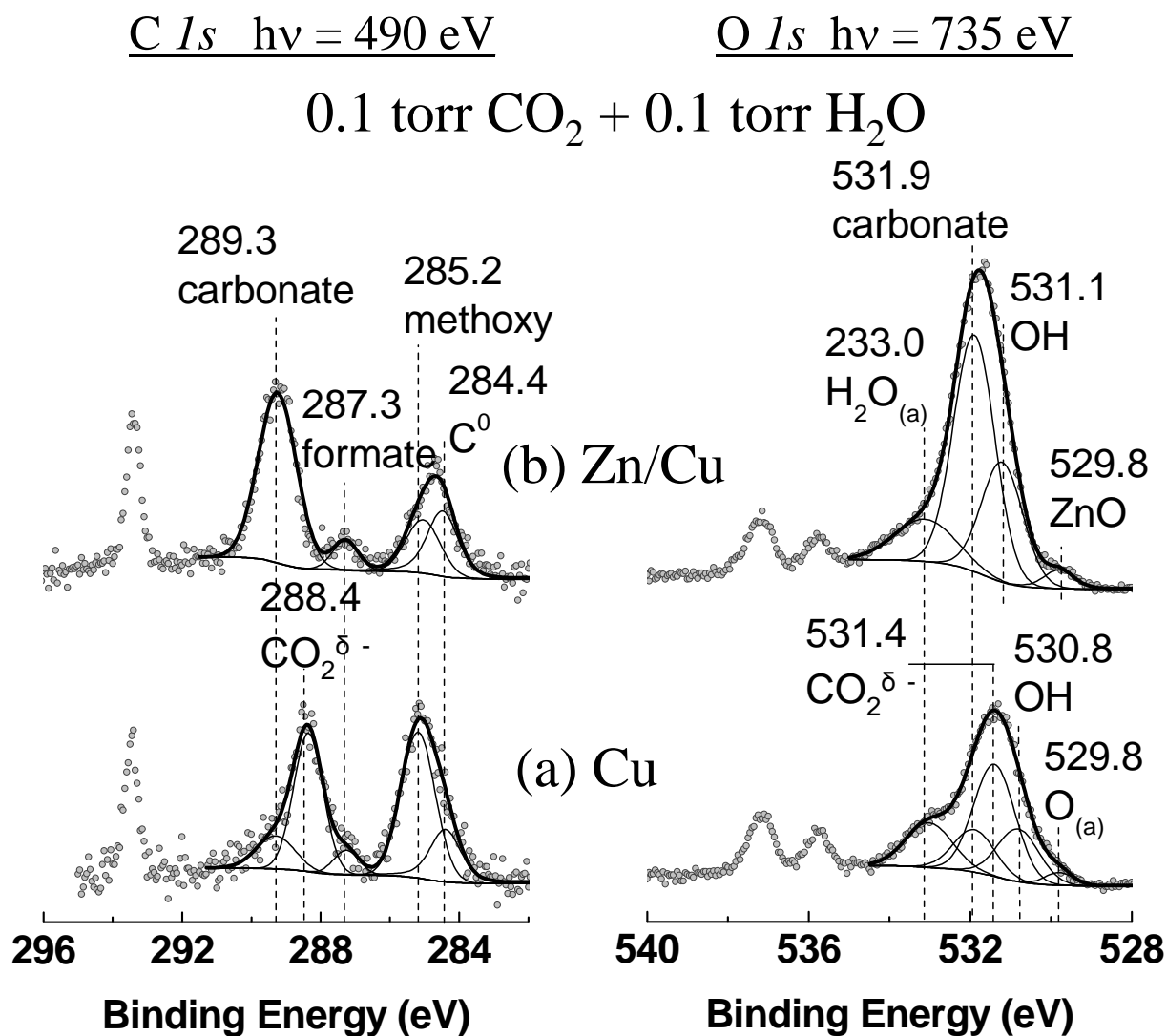


Figure 5. C 1s and O 1s XPS spectra of (a) pure Cu and (b) Zn/Cu (0.1 ML Zn) in the presence of 0.1 torr CO₂ + 0.1 torr H₂O at room temperature. Two new carbonaceous species, formate and methoxy are shown to form on both surfaces. The activated CO₂ and carbonate species present in pure CO₂ (figure 3) remain visible on each surface. In addition, molecularly adsorbed H₂O is also observed in both spectra.

In the O *1s* region, in addition to the peaks observed in the presence of pure CO₂, a new broad peak, with binding energy of 533.0 eV, is observed on both Cu and Zn/Cu surfaces. We assign this peak to adsorbed molecular H₂O.¹⁸ Unfortunately, we are not able to resolve the O *1s* peaks for methoxy and formate. According to the literature,²¹⁻²³ the binding energy of O *1s* for methoxy is between 530.2-530.9 eV and that for formate is ~531.4 eV. These peaks therefore strongly overlap with those of other major species, i.e., OH and/or carbonate.

In the highest binding energy peaks observed in the C and O *1s* regions are due to gas phase CO₂ (294 eV and 537 eV) and H₂O (536 eV).

Discussion

The formation of chemisorbed, negatively charged CO₂^{δ-} on the Cu surface has been proposed and identified based on spectroscopic studies, such as surface enhanced Raman (SERS)¹⁰ and X-ray photoelectron spectroscopy (XPS).^{6,7} For example CO₂^{δ-} on a cold deposited Cu film gives peaks at 767 cm⁻¹ (bending mode δ(OCO)) and 1182 cm⁻¹ (symmetric stretch mode ν_s(OCO)) in the SER spectrum,¹⁰ which is significantly different from the vibrational modes of neutral CO₂ (644 and 1261 cm⁻¹, correspondingly). Unfortunately there is a wide range of XPS binding energy values for C *1s* and O *1s* for CO₂^{δ-} reported in the literature. In this study, we found that the binding energies of C *1s* and O *1s* for CO₂^{δ-} are 288.4 and 531.4 eV, respectively, close to the values determined by Copperthwaite *et al.*⁶

Dissociation of CO₂ to CO and adsorbed oxygen on Cu is less likely under the current experimental conditions (at room temperature and at 0.1 torr CO₂) although it has been shown to be a rate-limiting step for the reverse water gas shift reaction over Cu.^{14,24,25} According to the study of Nakamura *et al.*,¹⁴ dissociation of CO₂ was observed on Cu(110) at high temperatures (400-600 K) and at high pressures (65-650 Torr) with dissociation probabilities of ~10⁻⁹-10⁻¹¹ (per collision with the surface). This rules out the possibility that reactions such as CO₂(g) → CO(g) + O(a) and CO₂ + O(a) → CO₃(a) take place with any significant rate on Cu, and indicates the existence of other reaction channels for forming carbonate and chemisorbed oxygen.

In fact, it has been suggested that the activation of CO₂ to CO₂^{δ-} is a crucial step since this activated species acts as a precursor for all reactions involving CO₂ on Fe²⁶⁻²⁹ and Pd^{30,31}. On the Cu surface, it has also been suggested that CO₂^{δ-} can lead to carbonate formation via the reaction:^{6,7}



The carbonate species observed on Cu in the presence of 0.1 torr CO₂ at room temperature is thus potentially the result from such reaction. On clean Cu this reaction does not proceed to completion in our pressure and temperature conditions, as shown by the observed ratio of CO₂^{δ-} to CO₃ of approximately 4:1 (Figure 3).

Addition of 0.1 ML Zn to the Cu surface leads to a substantial growth of carbonate and the concomitant depletion of CO₂^{δ-}, in effect strongly shifting reaction (1) to the right side. Although the detailed mechanism is not clear our results show that Zn facilitates carbonate formation, perhaps acting as a catalyst in a similar way as observed for alkali metals such as Na,⁷ K,¹⁰ and Cs.^{32,33}

The carbonate can undergo further de-oxygenation or reduction:^{6,7}



Indeed we observed a substantial C peak at 284.4 eV on either Cu or Zn/Cu in the presence of CO₂, supporting the occurrence of reaction (2). The O(a) formed from the reaction (2) should contribute to the O 1s peak at 529.8 eV, which has distinct fates on Cu and Zn/Cu: in the case of Cu it remains as chemisorbed oxygen whereas on Zn/Cu it oxidizes Zn to form ZnO.

Formation of CO₂^{δ-} involves charge transfer from the copper substrate into the 2π_u orbital of the molecule and thus the work function of the substrate will influence the activation of the adsorbate. Bartos *et al.* observed that CO₂^{δ-} is formed on clean surfaces where the work function is below 5 eV.³⁴ Notably, the work function of Cu surface (polycrystalline) has been determined to be 4.46 ± 0.03 eV,³⁵ and therefore it should be capable of activating CO₂. On the other hand, the work function of Cu₂O is 5.2 eV, consistent with the observation that Cu₂O is originally inactive towards CO₂. However, there is the possibility that photons or photoelectrons generated during the XPS data collection could assist

$\text{CO}_2^{\delta-}$ formation. Such photoinduced carbonate formation is quite similar to the observation that x-ray induces CO_2 activation to $\text{CO}_2^{\delta-}$ on the unreactive Cu(100) at low temperatures.⁷

It is clear that one of the roles of H_2O is to provide hydrogen for the formation of methoxy and formate species. Formate could be formed by transfer of a hydrogen atom to $\text{CO}_2^{\delta-}$ or by hydrogenation of the carbonate, whereas methoxy formation is more complicated, requiring multiple steps.

In methanol synthesis, formate and methoxy have been suggested as intermediates on the Cu-Zn catalyst when a mixed feed of CO_2 and H_2 was used.³⁶ It was discussed that the adsorbed CO_2 is hydrogenated to formate species, which is further hydrogenated to methoxy.^{37,38} Clearly, we observed both formate and methoxy species on Cu and Zn/Cu when both CO_2 and H_2O are present in the gas phase with H_2O (instead of H_2) providing the hydrogen needed for the formation of hydrogenated species. While some of the surface species found in our room temperature study occur also in the methanol synthesis reaction, the present results should not be extrapolated without caution to the catalytic system where H_2 is used instead of H_2O and where the temperature is ~ 500 K.

The present characterization of the chemical nature of Cu surfaces in the presence of CO_2 and H_2O at room temperature is relevant in the field of electric motors since Cu is a widely used material in both rotor and brush electrodes (sometimes also containing Zn), and because the motors operate often in environments containing CO_2 and H_2O . The oxide film, carbonate, activated CO_2 , formate and methoxy are all important surface species that might play a substantial role in the resistivity, corrosion and wear properties of Cu electric motors and thus deserve to be examined in detail to understand and improve their electrical and mechanical properties. In view of the chemical transformations induced by the x-rays described above, which most likely involve secondary electrons at very low energies, it is possible that similar reactions can take place in the electrode surfaces of the motors, due to the high electrical currents circulating across the interfaces. The formation of carbonates, formates and methoxy, can be strongly affected by the strength of the electric field and polarity across electrodes. Our results provide the first spectroscopic view of the rich chemistry that can occur at electrode surfaces and its connection to the

voltage drop and polarity across the electrodes. These and more extended studies can provide a better understanding of the complex chemistry and tribology of electrical contacts.

Conclusions

The surface chemistry of Cu₂O, Cu and Zn/Cu system in the presence of CO₂ at room temperature has been investigated *in-situ* using x-ray photoelectron spectroscopy near ambient conditions of temperature and pressure. We found Cu₂O to be inactive towards CO₂ adsorption at room temperature, while clean Cu is capable of activating CO₂ to negatively charged CO₂^{δ-} species, which can further convert to carbonate. Carbonate undergoes de-oxygenation or reduction, yielding C^{0(a)} and chemisorbed oxygen on the surface. The presence of 0.1 ML Zn on Cu facilitates carbonate formation while depleting the concentration of CO₂^{δ-} on the surface. In addition to the species observed in pure CO₂, methoxy and formate are formed when H₂O is coadsorbed, which then provides the hydrogen needed for the reaction.

Acknowledgements

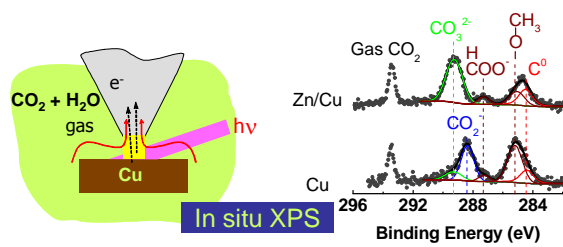
This work was supported by the Director, Office of Science, Office of Basic Energy Sciences, the Chemical Sciences, Geosciences, and Biosciences Division under the Department of Energy Contract No. DE-AC02-05CH11231 and the Office of Naval Research through the University of Wisconsin, Milwaukee under contract No. 446541. A.V. acknowledges financial support from the NANOS postdoctoral program, Generalitat de Catalunya and the Ramon y Cajal Program of the Ministerio de Educación y Ciencia, Spain. T. H. acknowledges the financial support from the Ramon Areces Foundation.

References

- (1) Boyer, L.; Noel, S.; Chabrierie, J. P. *Wear* **1987**, *116*, 43.

- (2) Slade, P. G. *Electrical Contacts: Principles and Applications*, Marcel Dekker: New York, 1999.
- (3) Chinchin, G. C.; Spencer, M. S.; Waugh, K. C.; Whan, D. A. *J. Chem. Soc. Faraday Trans.* **1987**, *83*, 2193.
- (4) Salmi, T.; Hakkarainen, R. *Appl. Catal.* **1989**, *49*, 285.
- (5) Waugh, K. C. *Catal. Today* **1992**, *15*, 51.
- (6) Copperthwaite, R. G.; Davies, P. R.; Morris, M. A.; Roberts, M. W.; Ryder, R. A. *Catal. Lett.* **1988**, *1*, 11.
- (7) Browne, V. M.; Carley, A. F.; Copperthwaite, R. G.; Davies, P. R.; Moser, E. M.; Roberts, M. W. *Appl. Surf. Sci.* **1991**, *47*, 375.
- (8) Carley, A. F.; Chambers, A.; Davies, P. R.; Mariotti, G. G.; Kurian, R.; Roberts, M. W. *Faraday Discuss.* **1996**, *105*, 225.
- (9) Rasmussen, P. B.; Taylor, P. A.; Chorkendorff, I. *Surf. Sci.* **1992**, *270*, 352.
- (10) Pohl, M.; Otto, A. *Surf. Sci.* **1998**, *406*, 125.
- (11) Campbell, C. T.; Daube, K. A.; White, J. M. *Surf. Sci.* **1987**, *182*, 458.
- (12) Krause, J.; Borgmann, D.; Wedler, G. *Surf. Sci.* **1996**, *347*, 1.
- (13) Fu, S. S.; Somorjai, G. A. *Surf. Sci.* **1992**, *262*, 68.
- (14) Nakamura, J.; Rodriguez, J. A.; Campbell, C. T. *J. Phys. Con. Matt.* **1989**, *1*, SB149.
- (15) Bluhm, H.; Havecker, M.; Knop-Gericke, A.; Kleimenov, E.; Schlogl, R.; Teschner, D.; Bukhtiyarov, V. I.; Ogletree, D. F.; Salmeron, M. *J. Phys. Chem. B* **2004**, *108*, 14340.
- (16) Briskman, R. N. *Sol. Energy Mater. Sol. Cells* **1992**, *27*, 361.
- (17) Ogletree, D. F.; Bluhm, H.; Lebedev, G.; Fadley, C. S.; Hussain, Z.; Salmeron, M. *Rev. Sci. Instr.* **2002**, *73*, 3872.
- (18) Yamamoto, S.; Andersson, K.; Bluhm, H.; Ketteler, G.; Starr, D. E.; Schiros, T.; Ogasawara, H.; Pettersson, L. G. M.; Salmeron, M.; Nilsson, A. *J. Phys. Chem. C* **2007**, *111*, 7848.
- (19) Deng, X.; Herranz, T.; Weis, C. D.; Bluhm, H.; Salmeron, M. B. *J. Phys. Chem. C* **2008**, accepted.
- (20) Moretti, G.; Fierro, G.; Lojacono, M.; Porta, P. *Surf. Inter. Anal.* **1989**, *14*, 325.
- (21) Bukhtiyarov, V. I.; Prosvirin, I. P.; Tikhomirov, E. P.; Kaichev, V. V.; Sorokin, A. M.; Evstigneev, V. V. *React. Kinet. Catal. Lett.* **2003**, *79*, 181.
- (22) Gunther, S.; Zhou, L.; Havecker, M.; Knop-Gericke, A.; Kleimenov, E.; Schlogl, R.; Imbihl, R. *J. Chem. Phys.* **2006**, *125*, 114709.
- (23) Carley, A. F.; Owens, A. W.; Rajumon, M. K.; Roberts, M. W.; Jackson, S. D. *Catal. Lett.* **1996**, *37*, 79.
- (24) Ernst, K. H.; Campbell, C. T.; Moretti, G. *J. Catal.* **1992**, *134*, 66.
- (25) Ovesen, C. V.; Stoltze, P.; Norskov, J. K.; Campbell, C. T. *J. Catal.* **1992**, *134*, 445.
- (26) Behner, H.; Spiess, W.; Wedler, G.; Borgmann, D. *Surf. Sci.* **1986**, *175*, 276.
- (27) Freund, H.-J.; Behner, H.; B., B.; Wedler, G.; Kuhlenbeck, H.; M., N. *Surf. Sci.* **1987**, *180*, 550.
- (28) Pirner, M.; Bauer, R.; Borgmann, D.; Wedler, G. *Surf. Sci.* **1987**, *189*, 147.
- (29) Wedler, G.; Kiessling, W.; Borgmann, D. *Vacuum* **1990**, *41*, 93.
- (30) Wambach, J.; Odorfer, G.; Freund, H.-J.; Kuhlenbeck, H.; Neumann, M. *Surf. Sci.* **1989**, *209*, 159.
- (31) Wohlrab, S.; Ehrlich, D.; Wambach, J.; Kuhlenbeck, H.; Freund, H.-J. *Surf. Sci.* **1989**, *220*, 243.
- (32) Carley, A. F.; Roberts, M. W.; Strutt, A. J. *Catal. Lett.* **1994**, *29*, 169.
- (33) Rodriguez, J. A.; Clendening, W. D.; Campbell, C. T. *J. Phys. Chem. B* **1989**, *93*, 5238.
- (34) Bartos, B.; Freund, H.-J.; Kuhlenbeck, H.; Neumann, M. *Kinetics of interface reactions*, Springer: Berlin, 1987.
- (35) Anderson, P. A. *Phys. Rev.* **1949**, *76*, 388.
- (36) Saussey, J.; Lavalley, J. C. *J. Mol. Catal.* **1989**, *50*, 343.

92. (37) Nakamura, I.; Nakano, H.; Fujitani, T.; Uchijima, T.; Nakamura, J. *Surf. Sci.* **1998**, *402*,
- (38) Nakamura, J.; Choi, Y.; Fujitani, T. *Top. Catal.* **2003**, *22*, 277.



TOC graphic